



ELSEVIER

Journal of Alloys and Compounds 323–324 (2001) 567–571

Journal of  
ALLOYS  
AND COMPOUNDS

www.elsevier.com/locate/jallcom

# Semi-empirical and ab-initio calculations of the crystal field interaction in rare earth cuprates

M. Diviš<sup>a,\*</sup>, V. Nekvasil<sup>b</sup><sup>a</sup>Department of Electronic Structures, Charles University, Ke Karlovu 5, 121 16 Praha 2, Czech Republic<sup>b</sup>Institute of Physics, Czech Academy of Sciences, Cukrovarnická 10, 162 53 Praha 6, Czech Republic

## Abstract

Semi-empirical and ab-initio methods useful for theoretical investigations of the crystal field (CF) interaction in rare earth (RE) cuprates are described. Concrete calculations are performed for  $\text{Sm}_{1+x}\text{Ba}_{2-x}\text{Cu}_3\text{O}_{6+y}$ , a system providing detailed data on intermultiplet infrared-active CF transitions for  $\text{Sm}^{3+}$  ions on the regular  $D_{4h}$  symmetry sites as well as on the substituted  $C_{4v}$  symmetry Ba sites. Within this study, the main attention is paid to the second order CF parameters calculated using a parameter free first principles method based on the density functional theory (DFT). A general potential linearized augmented plane wave (LAPW) computational method is used to obtain the ground state charge density. The calculated value of  $B_{20} = 320 \text{ cm}^{-1}$  in  $D_{4h}$  symmetry sites of Sm is in a good agreement with the phenomenological value of  $282 \text{ cm}^{-1}$  obtained from a fit to infrared transmission spectroscopy data. For Sm in the  $C_{4v}$  symmetry sites, the DFT value of  $B_{20} = -227 \text{ cm}^{-1}$  together with the standard superposition model values,  $B_{40} = 24$ ,  $B_{44} = -331$ ,  $B_{60} = -427$  and  $B_{64} = 624 \text{ cm}^{-1}$ , allow us to interpret the main features of the available infrared absorption data. It is shown that the sign of the  $B_{20}$  in  $\text{SmBa}_2\text{Cu}_3\text{O}_{6+y}$ , positive in the regular sites and negative in the Ba sites, is governed by the shape of the crystal potential within the LAPW atomic sphere of Sm atom. © 2001 Elsevier Science B.V. All rights reserved.

**Keywords:** High- $T_c$  superconductors; Crystal and ligand fields, electronic band structure

## 1. Introduction

The crystal field (CF) interaction in high- $T_c$  copper oxide superconductors containing rare earth (RE) ions is of prime interest in studies using these ions as a noninteracting probe of local electric and magnetic fields [1,2]. The  $\text{RE}^{3+}$  ions in cuprates are either sandwiched between two “superconducting”  $\text{CuO}_2$  layers or adjacent to one of them. Their localized and strongly correlated 4f states are perturbed by the CF potential originating from the surrounding charge distribution. Experimentally, the CF excitations have been studied by the inelastic neutron scattering and the electronic Raman scattering. Numerical analyses of the experimental spectra allowed us to determine sets of parameters of the CF Hamiltonian in many of the p-type superconductors,  $\text{REBa}_2\text{Cu}_3\text{O}_{6+x}$ , and the n-type superconductors  $\text{RE}_{2-x}\text{Ce}_x\text{CuO}_4$ , as well as in their non-superconducting parent compounds (see e.g., Refs. [2,3] and references therein).

This work examines theoretical methods allowing us to

predict the CF parameters in cuprates. Concrete calculations are performed for  $\text{Sm}_{1+x}\text{Ba}_{2-x}\text{Cu}_3\text{O}_{6+y}$ , a system providing ample experimental data on the CF interaction. In particular, absorption bands corresponding to  $\text{Sm}^{3+}$  CF excitations have been observed recently in the  $y \sim 0$  compound by infrared spectroscopy and assigned to transitions from the lowest energy levels of the  ${}^6\text{H}_{5/2}$  multiplet to the  ${}^6\text{H}_{7/2}$ ,  ${}^6\text{H}_{9/2}$ ,  ${}^6\text{H}_{11/2}$ ,  ${}^6\text{H}_{13/2}$ ,  ${}^6\text{F}_{7/2}$  and  ${}^6\text{F}_{9/2}$  excited multiplets of  $\text{Sm}^{3+}$  ions on the regular rare earth sites as well as on the substituted Ba sites [4].

## 2. Theoretical methods

An interaction with the crystal field produced by the neighboring core charges and valence electronic charge density is the strongest perturbation of the free ion 4f shell state of trivalent RE ions in cuprates. The interaction Hamiltonian can be written as:

$$H_{\text{CF}} = \sum_{k,q} B_{kq} [C_q^{(k)} + C_{-q}^{(k)}] \quad (1)$$

where  $C_q^{(k)}$  transform as tensor operators under simulta-

\*Corresponding author. Tel.: +420-2-2191-1368; fax: +420-2-2491-1061.

E-mail address: divis@mag.mff.cuni.cz (M. Diviš).

neous rotation of the coordinates of all the f electrons.  $B_{kq}$  are the so-called CF parameters [5].

The principle aim of this work is an examination of the CF of  $\text{Sm}^{3+}$  at regular  $D_{4h}$  symmetry sites and at  $C_{4v}$  symmetry Ba sites in  $\text{Sm}_{1+x}\text{Ba}_{2-x}\text{Cu}_3\text{O}_6$ . In both cases the CF interaction can be described using Eq. (1), which contains five non-zero independent parameters  $B_{20}$ ,  $B_{40}$ ,  $B_{44}$ ,  $B_{60}$  and  $B_{64}$ . In this work their values are determined by combining different approaches. In regular Sm sites the unknown parameters  $B_{kq}$  were found solving numerically the *inverse secular problem*, where the experimental CF energy levels are considered to be the eigenvalues of the secular equation of  $H_{\text{CF}}$  [4].

For a prediction of the  $k=4$  and 6 CF parameters, the standard superposition model, proved to be efficient in the CF modeling [2], is available. The model, introduced to separate geometrical and physical information contained in the CF parameters, allowing us to describe the CF parameters  $B_{kq}$  in Eq. (1) in terms of intrinsic (pair) CF parameters  $b_k(R)$  where  $R$  denotes the distance between the RE and ligand ion as:

$$B_{kq} = \sum_i S_{kq}(i) \cdot b_k(R_i), \quad k = 4, 6 \quad (2)$$

where  $S_{kq}(i)$  is the geometrical factor determined by angular coordinates of ligands at the same distance  $R_i$ . A standard way of expressing the distance dependence of the intrinsic parameters is to assume the power law dependence:

$$b_k = b_k(R_0) \cdot (R_0/R)^t \quad (3)$$

The superposition model does not apply for the second order parameters where the long range electrostatic contribution appears to dominate what causes a breakdown of one of the postulates of the superposition model [6]. Therefore, to calculate  $B_{20}$  we use an ab-initio method recently applied to RE cuprates [7]. Within this method the electronic structure and related distribution of the ground state charge density are obtained from the first principle calculations based on the density functional theory (DFT). Exchange and correlation effects are treated within the local spin density approximation (LSDA) and the general gradient approximation (GGA) [8]. The scalar relativistic Kohn–Sham equations are used to obtain the selfconsistent single electron wave functions. The calculations described are performed using the full potential linearized augmented plane wave method (LAPW) implemented in the latest version of WIEN97 of the original WIEN code [9]. Atomic sphere radii of 2.8, 2.0, 1.9 and 1.5 a.u. are taken for Sm, Ba, Cu and O, respectively. Basis functions are represented by 1500 plane wave functions (more than 100 APW/atom) plus local orbitals of Sm (5s, 5p), Ba (5s, 5p), Cu (3p) and O (2s) semicore states, which lie less than 6 Ry below the Fermi level. A maximum of  $l=12$  was adopted for the expansion of the radial wave function. Inside the spheres,

the crystal potential and charge density are expanded into crystal harmonics up to the sixth order. For the Brillouin zone integrations, a tetrahedron method [9] with 40–50 special  $k$ -points is used. The remaining computational details are very similar to those in Ref. [10].

The Sm 4f states in the spherical part of the potential are treated as atomic-like core states (open-core treatment, see for example Ref. [11]). Sm in the compound studied is characterized by the integer occupation number  $N_{4f}=5$ . A similar approach was successfully used in the DFT calculations for  $\text{PrBa}_2\text{Cu}_3\text{O}_6$  [12]. The structural data from Ref. [13] were used in the following DFT-based calculations for  $B_{20}$ .

Within the DFT the parameter  $B_{20}$  of the CF Hamiltonian, Eq. (1), originating from the effective potential  $V$  inside the crystal, is written as

$$B_{20} = a_0^2 \int_0^\infty |R_{4f}(r)|^2 V_0^2(r) r^2 dr \quad (4)$$

where the non-spherical component  $V_0^2(r)$  reflects besides the nuclear potentials and Hartree part of the inter-electronic interaction also the exchange correlation term which accounts for many particle effects. The radial wave function  $R_{4f}$  describes the radial shape of the localized 4f charge density of the  $\text{Sm}^{3+}$  ion in studied compounds. It is well known that the use of self-consistent “open core”  $R_{4f}$  leads to a poor description of the CF interaction. The reason is that the so-called “self-nteraction” potential felt by a localized 4f electron is not correctly treated within the LSDA [11]. Therefore, the present study uses the value of the  $R_{4f}$  in Eq. (4) resulting from the self interaction corrected (SIC) LSDA atomic calculations with occupation numbers of the valence electrons of the Sm (6s, 5d, 6p) fixed to their values obtained in the self consistent LSDA calculations in a given Sm compound. This approach [14] was found to give the 4f charge density which is very close to that obtained from a more rigorous DFT band calculation which includes SIC for the 4f states directly [11]. We note that our approach includes anisotropic charge polarization.

To calculate  $V_0^2(r)$  we rewrote the right hand side of Eq. (4) as a sum of two contributions:

$$B_{20} = a_0^2 \left( \int_0^{R_{MT}} |R_{4f}(r)|^2 U_0^2(r) r^2 dr + \int_{R_{MT}}^\infty |R_{4f}(r)|^2 W_0^2(r) r^2 dr \right) \quad (5)$$

where  $U_0^2(r)$  and  $W_0^2(r)$  are respectively the components of the effective potential inside the atomic sphere with radius  $R_{MT}$  and in the interstitial region. The term  $U_0^2(r)$  is readily available from WIEN97 code since the LAPW method uses the expansion of the potential in terms of linear combination of radial functions times spherical harmonics  $Y_{kq}(\vartheta, \phi)$  inside the atomic sphere. In the interstitial region a plane

wave expansion is used. In contrast to Ref. [7] the term  $W_0^2(r)$  is now obtained using the exact transformation of the interstitial plane wave representation of potential into the spherical Bessel functions. The conversion factor  $a_0^2 = \sqrt{5/4\pi}$  establishes the relation between the LAPW symmetrized spherical harmonic and the real Tesseral harmonic which transforms in the same way as tensor operator  $C_0^{(2)}$  in Eq. (1).

It follows from our earlier applications of the current DFT method in oxidic insulators [7] that this approach is not suitable for CF parameters of rank 4 and 6. This fact points to the importance of hybridization (covalency) between 4f and oxygen ligand 2s, 2p wave functions, which is neglected in our present DFT calculations. The hybridization contributions are more important to the values of rank 4 and 6 CF parameters than for the rank 2 as it was shown by Newman (see Ref. [15], Table 12, p. 235). Therefore in the present work, we use DFT based calculations for the CF parameters rank 2 only.

### 3. Results and discussion

We first describe our results for Sm regular sites in  $\text{SmBa}_2\text{Cu}_3\text{O}_6$ . Calculated electronic band structures and densities of states (DOS) in this compound are very similar to those in  $\text{YBa}_2\text{Cu}_3\text{O}_7$  (see Fig. 1). Data for the latter compound were found to agree very well with the available LAPW data [16]. We note that the Fermi level ( $E_F$ ) falls just above the high DOS region for both systems studied: it lies 0.1 and 0.2 eV above a sharp peak of the hybridized O(1)–O(4) states in  $\text{YBa}_2\text{Cu}_3\text{O}_7$  and  $\text{SmBa}_2\text{Cu}_3\text{O}_6$ , respectively. The value of  $N(E_F) = 6.15$  (states/eV) for  $\text{YBa}_2\text{Cu}_3\text{O}_7$  compares well with available values ranging from 5.54 to 6.8 [16]. The total occupied valence bandwidth is 6.9 eV for both systems studied. The small differences around  $-6$  eV,  $-3$  eV and above 2 eV are connected with oxygen (0, 0.5, 0) states which are missing in  $\text{SmBa}_2\text{Cu}_3\text{O}_6$  and with hybridization of Sm–5d (Y–4d) states with remaining Cu–3d, Cu–4s, O–2p and Ba–6s valence states.

To avoid the problem of selfinteraction, inherent to any approach treating the localized 4f states [11,17,18], we used a standard approximation namely that the aspherical terms in the total crystal potential entering Eqs. (4) and (5) have been calculated for systems with the spherical symmetric Sm 4f shell. The resulting CF parameters are thus not influenced by the aspherical part of the 4f electron density. Within this approach we avoid the need to consider the impact of the change of the valence states upon reorientation of the 4f charge density. At the same time we took into account the asphericity of Sm 5p electrons treating them as the local orbitals [18].

Using Eq. (5) for Sm in the regular sites in  $\text{SmBa}_2\text{Cu}_3\text{O}_{6+y}$ ,  $y=0, 1$ , as described in the previous section, we obtained the respective values of  $B_{20} = 320$

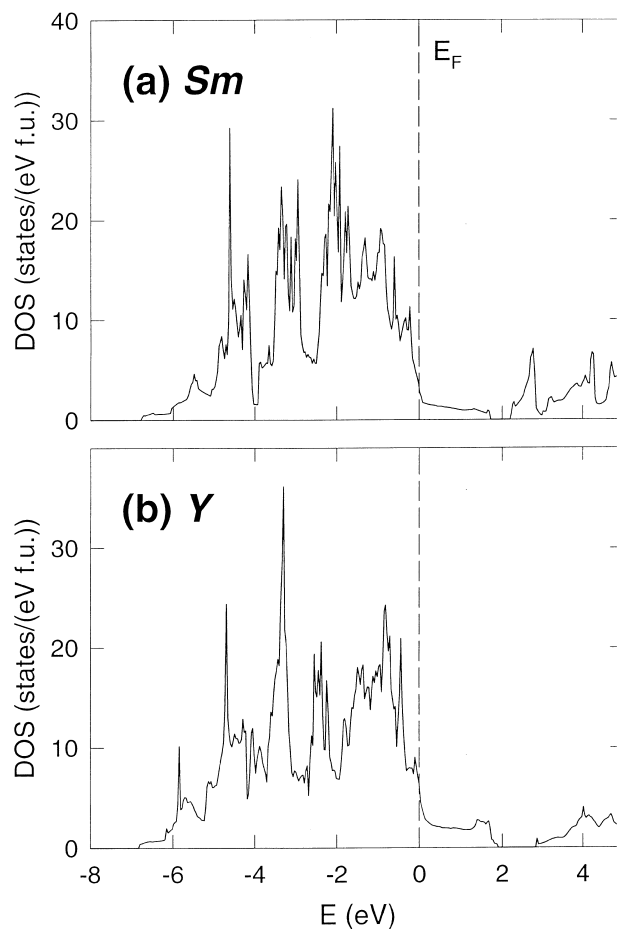


Fig. 1. Total density of electron states (DOS) of  $\text{SmBa}_2\text{Cu}_3\text{O}_6$  (a) and  $\text{YBa}_2\text{Cu}_3\text{O}_7$  (b). The Fermi level ( $E_F$ ) is set to the zero of the energy scale.

$\text{cm}^{-1}$  and  $B_{20} = 526 \text{ cm}^{-1}$  ( $y=1$ ). The former value is in very good agreement with the phenomenological value of  $282 \text{ cm}^{-1}$  (Table 1). Another check of our method is provided by similar calculations for  $\text{NdBa}_2\text{Cu}_3\text{O}_{6+y}$ ,  $y=0$ . In this case we found  $B_{20} = 412 \text{ cm}^{-1}$  which should be compared with the best fit value of  $380 \text{ cm}^{-1}$  [19]. Thus our method reproduces correctly not only the positive sign of  $B_{20}$  but also the experimental finding:  $B_{20}(\text{NdBa}_2\text{Cu}_3\text{O}_{6+y}) > B_{20}(\text{SmBa}_2\text{Cu}_3\text{O}_{6+y})$ . The relevant calculated radial charge distribution  $R_{4f}(r)$ , component of the crystal potential  $V_0^2(r)$  and  $I(r)$ , representing the integ-

Table 1

CF parameters (in  $\text{cm}^{-1}$ ) in  $\text{SmBa}_2\text{Cu}_3\text{O}_6$  obtained from a fit to IR measurements for  $\text{Sm}^{3+}$  ions on the regular ( $D_{4h}$  symmetry) site [4] and calculated using the superposition model and DFT based ab-initio methods for  $\text{Sm}^{3+}$  on the Ba sites ( $C_{4v}$ )

Parameter	$D_{4h}$ site	$C_{4v}$ site
$B_{20}$	282	-227
$B_{40}$	-2481	24
$B_{44}$	1307	-331
$B_{60}$	321	-427
$B_{64}$	1931	624

rand on the right hand side of Eq. (5) are for  $\text{SmBa}_2\text{Cu}_3\text{O}_{6+y}$  shown in Fig. 2a–c, respectively. To further test the reliability of our DFT-based CF calculations, we have also performed non spin-polarized LSDA calculations including spin-orbit interactions for valence electrons, spin-polarized LSDA calculations (4f electrons as spin-polarized core states) and non spin-polarized GGA calculations. The relative change of the resulting CF parameter  $\text{d}B_{20}/B_{20}$  was found to be less than 10% in all above mentioned cases.

To estimate the fourth and sixth order parameters of Hamiltonian (1) for  $\text{Sm}^{3+}$  entering the Ba sites we used the superposition model, Eqs. (2) and (3), considering the available intrinsic model parameters  $b_k$  and  $t_k$  [2] and structural data in  $\text{SmBa}_2\text{Cu}_3\text{O}_{6+y}$  [13]. The same structural data were used in the following DFT-based calculations for  $B_{20}$ . The task was to solve the case when the impurity Sm atom enters the  $(0.5, 0.5, z_{\text{Ba}})$  positions in the otherwise ideal  $\text{SmBa}_2\text{Cu}_3\text{O}_6$  crystal structure. This task requires construction of very large supercells, at least 30 times

larger than the elementary cell in the ideal structure  $\text{SmBa}_2\text{Cu}_3\text{O}_6$ , i.e., it includes several hundreds of atoms. The general potential DFT calculations reported so far do not go beyond  $\sim 100$  atoms in the elementary cell. To calculate  $B_{20}$  in Ba sites we have thus introduced the artificial crystal structure  $\text{Ba}(\text{Ba}, \text{Sm})_2\text{Cu}_3\text{O}_6$  in which Sm is in  $(0.5, 0.5, z_{\text{Ba}})$  positions and Ba occupies  $(0.5, 0.5, 1 - z_{\text{Ba}})$  and  $(0.5, 0.5, 0.5)$  positions. The important feature of this artificial structure is that the nearest and the next nearest neighbor coordinations are the same as in the ideal supercell. In particular, for the Sm atom located in the  $(0.5, 0.5, z_{\text{Ba}})$  position there are four oxygens O(1) in the same distance  $R[\text{Sm}-\text{O}(1)]=278$  pm and four oxygens O(2),  $R[\text{Sm}-\text{O}(2)]=289$  pm; the next nearest neighbor copper shell is composed of four Cu(2),  $R[\text{Sm}-\text{Cu}(2)]=337$  pm and four Cu(1),  $R[\text{Sm}-\text{Cu}(1)]=355$  pm. The local point group symmetry of  $(0.5, 0.5, z_{\text{Ba}})$  position differs in the ideal and artificial structures and the coordination shells start to differ beyond  $R=360$  pm. As a further test we also performed the DFT calculations for the artificial structures  $\text{Sm}(\text{Ba}, \text{Sm})_2\text{Cu}_3\text{O}_6$  and  $\text{La}(\text{Ba}, \text{Sm})_2\text{Cu}_3\text{O}_6$ . The corresponding DFT ground state charge densities are assumed to represent the limiting cases for the problem studied. Such numerical simulations have shown, however, that these differences do not influence the final value of  $B_{20}$  considerably [ $B_{20}$  remains negative and equals  $B_{20} = -531 \text{ cm}^{-1}$  and  $B_{20} = -484 \text{ cm}^{-1}$  in  $\text{Sm}(\text{Ba}, \text{Sm})_2\text{Cu}_3\text{O}_6$  and  $\text{La}(\text{Ba}, \text{Sm})_2\text{Cu}_3\text{O}_6$ , respectively so  $\text{d}B_{20}/B_{20}$  was found to be less than 15% in both cases studied]. Therefore, we consider our value of  $B_{20} = -227 \text{ cm}^{-1}$ , obtained using Eq. (5) for the artificial structure  $\text{Ba}(\text{Ba}, \text{Sm})_2\text{Cu}_3\text{O}_6$ , a meaningful estimate for this parameter for Sm in Ba sites in  $\text{SmBa}_2\text{Cu}_3\text{O}_6$ . The relevant calculated radial charge distribution  $R_{4f}(r)$ , component of the crystal potential  $V_0^2(r)$  and  $I(r)$ , representing the integrand on the right hand side of Eq. (5), are shown in Fig. 3a–c respectively. The above mentioned CF parameters in Sm-compounds are summarized in Table 1. Those in the third column were found to provide a meaningful prediction for the CF spectra in substituted Ba sites [4].

To be noted is the difference in sign between  $B_{20}$  in the regular and Ba sites which are connected within our approach with a difference in the occupation of the  $p_x$ ,  $p_y$  and  $p_z$  orbitals in the 5p and 6p valence shells as well as of the  $d_{z^2}$ ,  $d_{x^2-y^2}$ ,  $d_{xy}$ ,  $d_{xz}$  and  $d_{yz}$  orbitals in the 5d valence shell. Significant contribution to  $B_{20}$  from charges within the atomic sphere is proportional to the quantities  $\Delta N_p$  and  $\Delta N_d$  which are functions of the occupation numbers  $n$ :  $\Delta N_p = 1/2(n_x + n_y) - n_z$  and  $\Delta N_d = n_{x^2-y^2} + n_{xy} - 1/2(n_{xz} + n_{yz}) - n_{z^2}$  [20]. In our case we have obtained  $\Delta N_p$  equal to  $-0.008$  and  $0.011$  electrons and  $\Delta N_d$  equal to  $-0.017$  and  $-0.001$  electrons for  $\text{Sm}^{3+}$  ion in the regular and Ba sites, respectively.

In conclusion, we note that the above described combined semi-empirical and ab-initio approach provides a useful tool in studies examining the nature of the doping

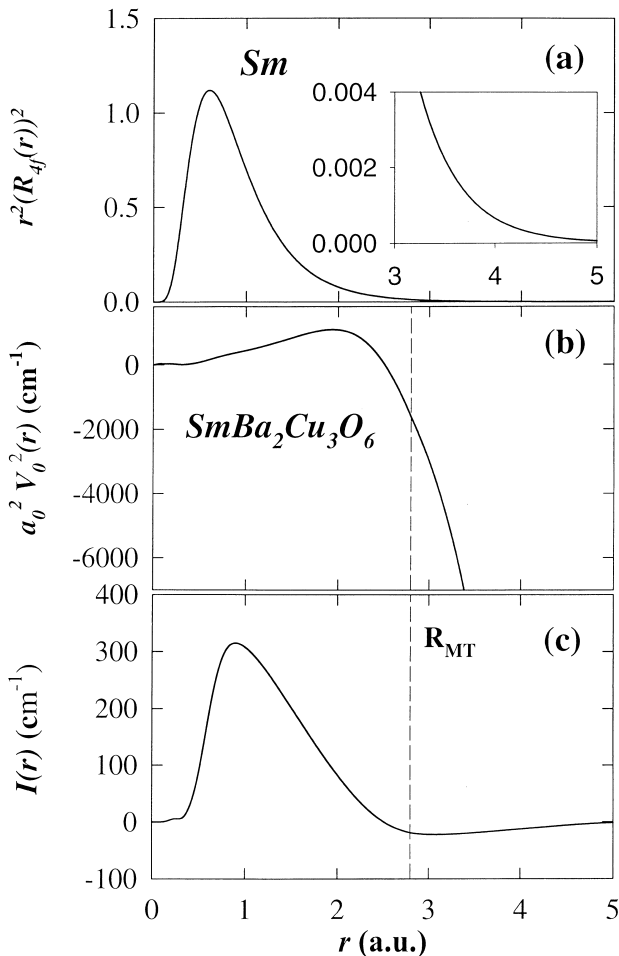


Fig. 2. Calculated radial charge density of 4f electrons  $R_{4f}(r)$  for Sm in the  $(0.5, 0.5, 0.5)$  position (a), the  $a_0^2 V_0^2(r)$  component of the total crystal potential (b) and the integrand  $I(r)$  on the right hand side of Eqs. (4) and (5) (c).

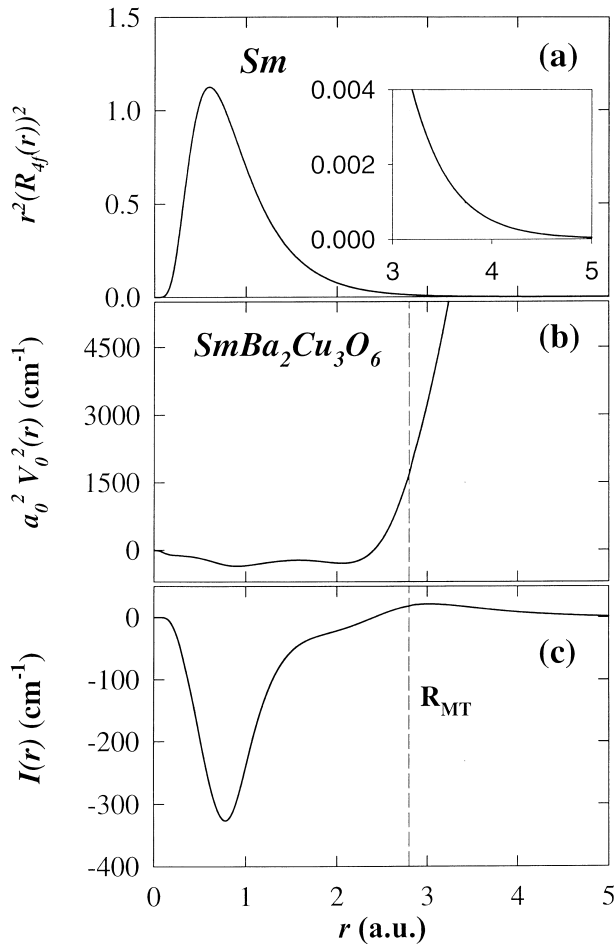


Fig. 3. Calculated radial charge density of 4f electrons  $R_{4f}(r)$  for Sm in the (0.5, 0.5,  $z_{\text{Ba}}$ ) position (a), the  $a_0^2 V_0^2(r)$  component of the total crystal potential (b) and the integrand  $I(r)$  on the right hand side of Eqs. (4) and (5) (c).

induced metallization of cuprates. Among others, it may help to decide the nature of the observed change of the CF at RE sites associated with the doping-induced charge transfer into the  $\text{CuO}_2$  planes [21–24].

### Acknowledgements

M.D. and V.N. gratefully acknowledge the Grant Agency of the Czech Republic for its Grants No. 202/00/1602 and

202/99/184 and M.D. gratefully acknowledges the Grant Agency of Charles University for its Grant No. 145/2000/B-FYZ.

### References

- [1] A. Furrer, in: L.C. Gupta, M.S. Multani (Eds.), *Frontiers in Solid State Sciences, Selected Topics in Superconductivity*, Vol. 1, World Scientific, Singapore, 1993, p. 349.
- [2] V. Nekvasil, M. Diviš, G. Hilscher, E. Holland-Moritz, *J. Alloys Comp.* 225 (1995) 578.
- [3] T. Strach, T. Ruf, M. Cardona, C.T. Lin, S. Jandl, V. Nekvasil, D.I. Zhigunov, S.N. Barilo, S.V. Shiryayev, *Phys. Rev. B* 54 (1996) 4276.
- [4] D. Barba, S. Jandl, A.A. Martin, C.T. Lin, M. Cardona, V. Nekvasil, M. Maryško, M. Diviš, T. Wolf, *Phys. Rev. B* 63 (2001) 054528.
- [5] B.G. Wybourne, *Spectroscopic Properties of Rare Earths*, Wiley, New York, 1965.
- [6] D.J. Newman, B. Ng, *Rep. Prog. Phys.* 52 (1989) 699.
- [7] M. Diviš, V. Nekvasil, J. Kuriplach, *Physica C* 301 (1998) 23.
- [8] J.P. Perdew, S. Burke, M. Ernzerhof, *Phys. Rev. Lett.* 77 (1996) 3865.
- [9] P. Blaha, K. Schwarz, J. Luitz, WIEN97, Vienna University of Technology, 1997, Improved and updated Unix version of the original copyrighted WIEN-code by P. Blaha, K. Schwarz, P. Sorantin, S.B. Trickey, *Comput. Phys. Commun.* 59 (1990) 399.
- [10] K. Schwarz, C. Ambosch-Draxl, P. Blaha, *Phys. Rev. B* 42 (1990) 2051.
- [11] M. Richter, *J. Phys. D: Appl. Phys.* 31 (1998) 1017.
- [12] C. Ambosch-Draxl, P. Blaha, K. Schwarz, *J. Phys.: Condens. Matter* 6 (1994) 2347.
- [13] M. Guillaume, P. Allenspach, W. Henggeler, J. Mesot, B. Roessli, U. Staub, P. Fischer, A. Furrer, V. Trounov, *J. Phys.: Condens. Matter* 6 (1994) 7963.
- [14] P. Novák, *Phys. Stat. Sol. (b)* 198 (1996) 729.
- [15] D.J. Newman, *Adv. Phys.* 20 (1971) 197.
- [16] W.E. Pickett, *Rev. Mod. Phys.* 61 (1989) 433.
- [17] P. Novák, J. Kuriplach, *J. Magn. Magn. Mater.* 104–107 (1992) 1499.
- [18] K. Hummler, M. Fähnle, *Phys. Rev. B* 53 (1996) 3272.
- [19] A.A. Martin, T. Ruf, M. Cardona, S. Jandl, D. Barba, V. Nekvasil, M. Diviš, T. Wolf, *Phys. Rev. B* 59 (1999) 6528.
- [20] R. Coehorn, K.H.J. Buschow, *J. Appl. Phys.* 69 (1991) 5590.
- [21] A. Furrer, P. Allenspach, F. Fauth, M. Guillaume, W. Henggeler, J. Mesot, S. Rosenkranz, *Physica C* 235–240 (1994) 261.
- [22] S.J.L. Billinge, T. Egami, *Phys. Rev. B* 47 (1993) 14386.
- [23] S. Jandl, P. Richard, M. Poirier, V. Nekvasil, A.A. Nugroho, A.A. Menovsky, D.I. Zhigunov, S.N. Barilo, S.V. Shiryayev, *Phys. Rev. B* 61 (2000) 12882.
- [24] V. Nekvasil, S. Jandl, M. Cardona, M. Diviš, A.A. Nugroho, this issue.